



Enhanced Quadrature Hybrid Coupler Design for 5G N1 Band Using Defected Ground Structures

Rudy Fernandez, Amirul Luthfi, Syukri Yunus, Tiara Feryndita Astuti

Departemen Teknik Elektro, Universitas Andalas, Kampus Limau Manis, Padang 25166, Indonesia

ARTICLE INFORMATION

Received: November 21, 2025
 Revised: December 01, 2025
 Accepted: December 12, 2025
 Available online: December 12, 2025

KEYWORDS

Defected Ground Structures, Hybrid Coupler, 5G Networks, Bandwidth Enhancement, RF Design

CORRESPONDENCE

E-mail: rfernandez@eng.unand.ac.id

A B S T R A C T

This study addresses the performance limitations of conventional hybrid couplers used in sub-6 GHz 5G infrastructure, targeting the N1 band (1.92–2.17 GHz), and integrates Defected Ground Structure (DGS) technology. The objective is to enhance bandwidth, reduce return and isolation losses, and optimize phase coupling while maintaining cost-effectiveness using FR-4 epoxy substrates. A quadrature hybrid coupler was designed and optimized using microstrip line technology with DGS modifications. The study employed advanced electromagnetic simulation software to evaluate key performance parameters, including return loss, isolation loss, bandwidth, insertion loss, and phase coupling. The DGS-modified design was compared with a conventional coupler to quantify performance improvements. The DGS-modified coupler achieved significant enhancements across all performance metrics. Return loss improved to -23.17 dB, isolation loss to -44.39 dB, and bandwidth increased by 34%, reaching 693.2 MHz. Phase coupling also approached the ideal 90° with a deviation of only 2.56° , significantly outperforming the conventional design. However, the insertion loss increased slightly to -4.34 dB, reflecting a trade-off between bandwidth enhancement and efficiency that must be considered in practical implementations. Overall, the integration of DGS into hybrid coupler designs provides a practical and effective means of enhancing RF component performance for reliable 5G networks while maintaining low-cost fabrication. These results underscore the potential of DGS technology for developing scalable, application-oriented solutions for next-generation wireless communications.

INTRODUCTION

The transition to 5G technology represents a significant advancement in wireless communication, promising improvements in data speeds, reduced latency, and the ability to connect a larger number of devices. This transformation is central to the evolution of digital technologies, including the Internet of Things (IoT), Artificial Intelligence (AI), and smart cities. The enhanced capabilities of 5G are expected to revolutionize various sectors such as healthcare, transportation, and industrial automation, thereby shifting how these industries operate and interact with technology [1, 2]. The key enabler of 5G's performance improvements is its ability to operate across multiple frequency bands, including low, mid, and high bands, which is essential for meeting the diverse requirements of modern applications [3].

However, to fully realize the potential of 5G, addressing the challenges posed by the increasing complexity of network infrastructure and the need for more efficient radio frequency (RF) components is crucial. Among the critical elements of 5G infrastructure, antenna systems and RF circuits, particularly hybrid couplers, play a significant role in ensuring signal quality

and network reliability. Hybrid couplers, which divide or combine power between multiple ports while maintaining phase balance, are integral to beamforming networks such as the Butler Matrix [4]. These couplers enable precise power distribution control across antenna arrays, a fundamental aspect of Multiple Input Multiple Output (MIMO) systems that underpin 5G's high capacity and efficient spectrum use [5]. Despite extensive studies on hybrid couplers, conventional designs often exhibit limitations in terms of narrow bandwidth and size, particularly at the higher frequencies utilized in 5G applications [6].

The challenge of optimizing hybrid couplers for 5G is further complicated by the frequency range and propagation characteristics of the N1 5G band (1.92–2.17 GHz), which necessitate efficient signal processing and minimal signal loss [7]. Current designs often fail to meet the desired specifications for return loss, isolation loss, and bandwidth, particularly when implemented with compact substrates such as FR-4 epoxy [8]. This issue is exacerbated by the demand for low-cost, manufacturable solutions that do not compromise performance. Previous studies have explored various methods to enhance hybrid coupler performance, such as modifying coupler geometries and incorporating different materials; however, these

solutions often lack scalability and consistent performance in the context of 5G [9].

In recent years, integrating Defected Ground Structure (DGS) into hybrid couplers has emerged as a promising approach to address these limitations. DGS modifies the ground plane of the coupler, introducing high-impedance paths that improve bandwidth, reduce harmonic distortion, and enhance overall performance [4]. DGS has been successfully applied to various RF components, including filters and antennas, demonstrating significant bandwidth increases and size reductions without compromising efficiency [10]. However, despite these advancements, a notable gap remains in the literature regarding the use of DGS in hybrid couplers specifically designed for the 5G N1 band. Addressing this gap is crucial for enhancing the efficiency of 5G infrastructure, as it would improve power handling, minimize signal interference, and optimize spectrum use in urban environments where high device density presents significant challenges [11].

This study contributes to the state of the art by presenting a novel design and optimization of a Quadrature Hybrid Coupler for the 5G N1 band, incorporating a unique DGS configuration on an FR-4 epoxy substrate. The novelty lies in three main aspects: first, the coupler is specifically tuned for the 5G N1 band under cost and size constraints typical of practical deployments; second, the DGS pattern and its dimensions are optimized to address the trade-off between bandwidth enhancement and insertion loss, a design-space exploration often overlooked in existing works; third, comprehensive simulation-based analysis is conducted to evaluate real-world metrics such as return loss, isolation, insertion loss, phase coupling, and bandwidth using a low-cost substrate. By systematically comparing the proposed coupler with a conventional design, this study offers a differentiated perspective and fills a critical research gap in the design of application-specific, performance-balanced hybrid couplers. The findings suggest a scalable and economical pathway to implement high-performance couplers in next-generation wireless communication systems.

METHODS

This study presents the design, simulation, and optimization of a Quadrature Hybrid Coupler tailored for the 5G N1 band (1.92 GHz – 2.17 GHz), utilizing microstrip line technology with Defected Ground Structure (DGS) modifications. The primary objective was to enhance key performance parameters, including bandwidth, return loss, isolation loss, and phase coupling, while maintaining cost-effectiveness through the use of an FR-4 epoxy substrate.

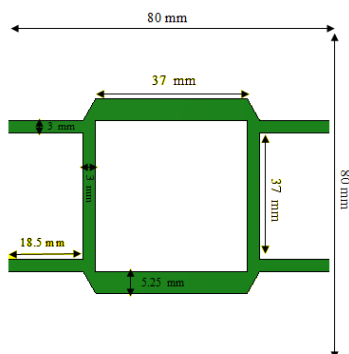


Figure 1. The initial design of the conventional couplers

The methodology commenced with the selection of FR-4 epoxy as the substrate, a widely used material in cost-sensitive RF applications due to its dielectric constant (ϵ_r) of 4.3, loss tangent ($\tan \delta$) of 0.0265, and thickness of 1.6 mm [14]. Initial design dimensions for the conventional hybrid coupler were derived using standard microstrip transmission line theory and synthesis equations, considering a center frequency of 2.045 GHz. These parameters are summarized in Table 1 and illustrated in Figure 1. This approach aligns with methodologies employed in previous studies involving planar couplers and RF components [12, 13, 14].

Table 1. Initial Dimensions of Hybrid Coupler (conventional design)

Dimension	(mm)
Shunt arm length (l_{50})	37
Shunt arm width (w_{50})	3
Series arm length (l_{35})	37
Series arm width (w_{35})	5.25
Feedline length (l_f)	18.5
Feedline width (w_f)	3
Thickness (t)	0.035

After establishing the conventional design, electromagnetic simulations were conducted to evaluate its performance. The DGS modification was then introduced to the ground plane in the form of rectangular slots, intended to generate high-impedance characteristics and disrupt current distribution, thereby improving bandwidth and isolation [15, 17]. This DGS-based enhancement technique follows principles validated in similar works on filters and antennas that demonstrate improved spectral characteristics and miniaturization without significantly increasing complexity [10, 17]. The configuration of the DGS used in this study is illustrated in Figure 2.

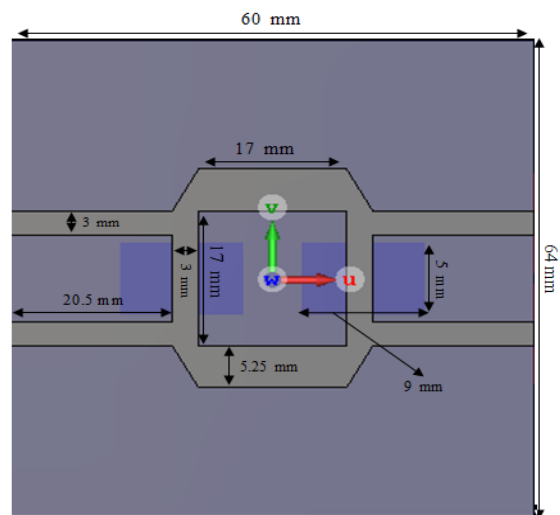


Figure 2. The Proposed Design of DGS-Modified Hybrid Coupler

A detailed optimization process followed, focusing on the physical dimensions of the microstrip arms (l_{50} and l_{35}), feed lines (l_f), and the DGS slot geometry. By iteratively adjusting these parameters, the design was fine-tuned to achieve ideal performance targets: return loss ≤ -10 dB, isolation loss ≤ -10 dB,

insertion loss ~ -3 dB, phase difference ~ 90°, and bandwidth ≥ 250 MHz [16].

Simulations were conducted using a full-wave electromagnetic solver widely employed in high-frequency RF circuit design. The extracted S-parameters (S11, S21, S31, S41) were used to compare the performance of both conventional and DGS-modified couplers. The observed improvements, visualized in Figures 4 through 10, substantiate the efficacy of DGS in hybrid coupler applications, as reported in earlier works [10, 17], and support the viability of this approach for compact and scalable 5G RF front-end implementations.

RESULTS AND DISCUSSION

The simulation of the Quadrature Hybrid Coupler for the 5G N1 band (1.92 – 2.17 GHz) was performed using a full-wave electromagnetic solver. Key metrics analyzed include return loss, isolation loss, insertion loss, phase coupling, and bandwidth.

Conventional Coupler Results

Table 2 summarizes the performance of the conventional coupler design at 2.045 GHz. The return loss (S11) was -8.69 dB and isolation loss (S41) was -9.63 dB, both failing to meet the target of ≤ -10 dB. Phase coupling between ports S21 and S31 was recorded at 111.11°, deviating significantly from the ideal 90° phase shift, and the insertion loss was relatively high at -6.43 dB. Figure 3 visualizes the return loss over the frequency band, indicating poor impedance matching beyond the optimal range.

Table 2. Simulation Results for Conventional Hybrid Coupler Design

Parameter	Desired Specification	Designed Results
Return Loss	≤ -10 dB	-8.69 dB
Isolation Loss	≤ -10 dB	-9.63 dB
Phase Coupling	90°	111,11°
Insertion Loss	-3 dB	-6,4362 dB
Coupling	-3 dB	-4,8292 dB

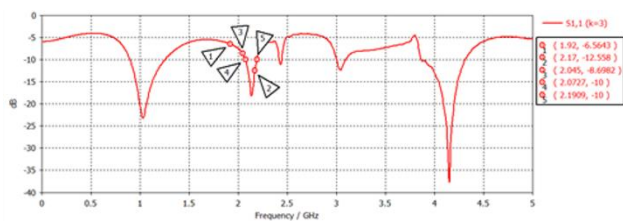


Figure 3. Simulation Results of Return Loss for Conventional Hybrid Coupler

These results are consistent with findings in the literature that highlight the challenges of maintaining performance using conventional hybrid couplers at higher frequencies [18, 20, 21].

DGS-Modified Coupler Results

The introduction of Defected Ground Structures (DGS) significantly improved the coupler's performance. Table 3 and

Figures 4–10 demonstrate these enhancements. The return loss improved to -23.17 dB (Figure 4), while isolation loss was greatly reduced to -44.39 dB (Figure 5), indicating a substantial reduction in signal leakage. Phase coupling was corrected to 87.44°, approaching the desired 90°, and insertion loss was reduced to -4.34 dB (Figure 6).

Table 3. Simulation Results for DGS-Modified Hybrid Coupler Design

Parameter	Target	DGS-Modified
Return Loss	≤ -10 dB	-23,17 dB
Isolation Loss	≤ -10 dB	-44,39 dB
Phase Coupling	90°	87.44°
Insertion Loss	-3 dB	-4.34 dB
Coupling	-3 dB	-3.33 dB
Bandwidth VSWR	≥ 250 MHz	693,2 MHz
Bandwidth Power	≥ 250 MHz	528.4 MHz
Balance		

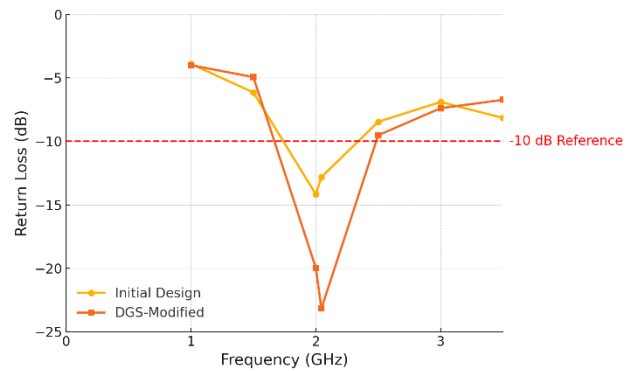


Figure 4. The Simulation Result of Return Loss in Comparison

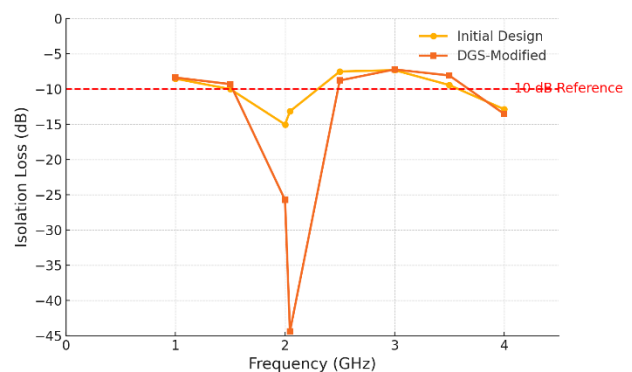


Figure 5. The Simulation Result of Isolation Loss in Comparison

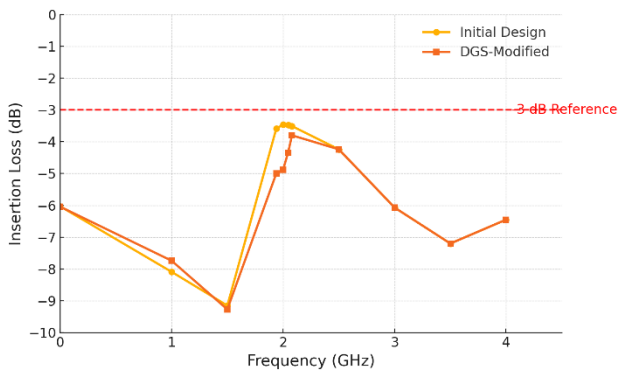


Figure 6. The Simulation Result of Insertion Loss in Comparison

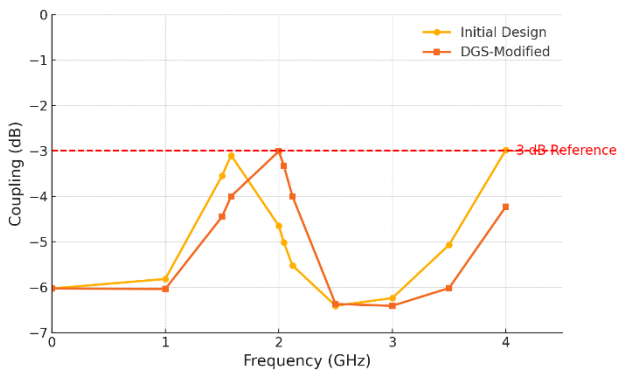


Figure 7. The Simulation Result of Coupling in Comparison

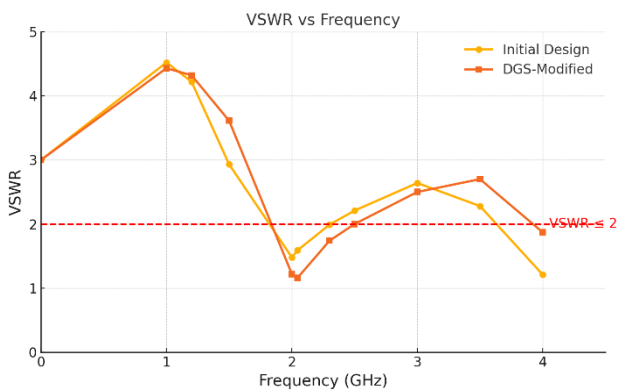


Figure 8. The Simulation Result of Bandwidth VSWR in Comparison

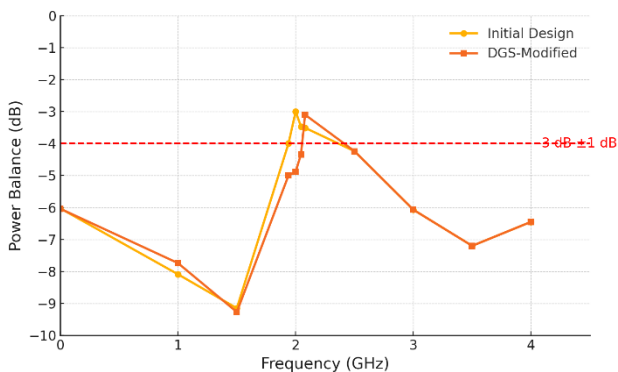


Figure 9. The Simulation Result of Bandwidth Power Balance from port 1 to port 2 in Comparison

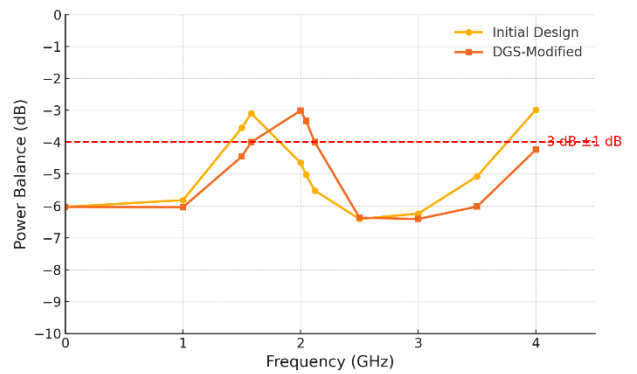


Figure 10. The Simulation Result of Bandwidth Power Balance from port 1 to port 3 in Comparison

Bandwidth also improved markedly: the VSWR bandwidth increased to 693.2 MHz (Figure 8), while the power balance bandwidth between ports 1–2 and 1–3 reached 528.4 MHz and 341.2 MHz, respectively (Figures 9 and 10). These outcomes confirm the DGS effectiveness in improving coupling uniformity and impedance matching.

Validation Limitations

Despite these promising outcomes, the design's validation relies exclusively on simulation. In RF and antenna engineering, such simulated performance often diverges from real-world behavior due to factors like fabrication tolerances, material inconsistencies, and connector losses. Therefore, without a fabricated prototype and empirical measurements, the reliability and applicability of these results remain uncertain. Future work should include prototyping and testing under practical conditions to validate the design.

Benchmark Comparison with Existing Designs

To contextualize the improvements, the proposed DGS-modified coupler can be compared with existing literature. For example, prior designs have reported return losses between -15 dB and -20 dB and bandwidths typically below 500 MHz using different substrates [13, 19, 22]. Compared to these, the proposed design achieves superior isolation and bandwidth while utilizing the low-cost FR-4 material.

Although insertion loss in this study is higher than the ideal -3 dB, the bandwidth and isolation enhancements present a valuable trade-off for applications where wider spectral coverage is essential. These comparisons suggest that the presented design offers a practical balance between cost efficiency and high-frequency performance, and can inform the further development of scalable RF components for 5G systems.

CONCLUSIONS

This study presented the design and electromagnetic simulation of a DGS-based quadrature hybrid coupler for 5G N1 band applications using an FR-4 epoxy substrate. The proposed coupler achieved the targeted performance enhancements, including improved impedance matching with a return loss of -23.17 dB, significantly reduced cross-talk with an isolation loss of -44.39 dB, a 34% increase in bandwidth to 693.2 MHz, and phase coupling close to 90°, thereby addressing the limitations of

the conventional design in terms of bandwidth, return loss, isolation loss, and phase balance. A remaining limitation is the insertion loss of -4.34 dB, slightly above the ideal -3 dB, suggesting that further optimization of the DGS configuration and substrate parameters, supported by prototype fabrication and measurements, is required to refine the trade-off between bandwidth enhancement and efficiency in practical 5G implementations.

ACKNOWLEDGMENT

This work was supported by Hibah Departemen Teknik Elektro No 60/UN.16.09.D/PL/2024.

REFERENCES

- [1] A. O. Watanabe, *et al.*, "A Review of 5G Front-End Systems Package Integration," *IEEE Transactions on Components Packaging and Manufacturing Technology*, vol. 11, no. 1, pp. 118–133, Dec. 2020, doi: <https://doi.org/10.1109/tcpmt.2020.3041412>.
- [2] F. Balteanu, "Circuits for 5G RF front-end modules," *International Journal of Microwave and Wireless Technologies*, vol. 15, no. 6, pp. 909–924, May 2023, doi: <https://doi.org/10.1017/s1759078722001295>.
- [3] A. Yacoub, M. Khalifa, and D. N. Aloï, "Wide Bandwidth Low Profile PIFA Antenna for Vehicular Sub-6 GHz 5G and V2X Wireless Systems," *Progress In Electromagnetic Research*, 109, 257–273, 2021, <https://doi.org/10.2528/PIERC21010609>.
- [4] G. N. Alsath and M. Kanagasabai, "Defected microstrip structure-based near-end and far-end crosstalk mitigation in high-speed PCBs for mixed signals | Emerald Insight," *Microelectronics International*, vol. 41, no. 1, pp. 16–25, 2022, doi: <https://doi.org/10.1108/MI>.
- [5] L. Kuai *et al.*, "A N260 Band 64 Channel Millimeter Wave Full-Digital Multi-Beam Array for 5G Massive MIMO Applications," *IEEE Access*, vol. 8, pp. 47640–47653, Jan. 2020, doi: <https://doi.org/10.1109/access.2020.2978070>.
- [6] M. Eid, H. Ibrahim, and T. Abouelnaga, "A Classification and Comparative Overview of CMOS Radio-Frequency Power Amplifiers," *Industrial Technology Journal*, vol. 0, no. 0, Oct. 2023, doi: <https://doi.org/10.21608/itj.2023.213588.1000>.
- [7] K. R. Mahmoud and A. M. Montaser, "Design of Compact mm-wave Tunable Filter Using Capacitor Loaded Trapezoid Slots in Ground Plane for 5G Router Applications," *IEEE Access*, vol. 8, pp. 27715–27723, Jan. 2020, doi: <https://doi.org/10.1109/access.2020.2971606>.
- [8] S. Shukla and S. Mukherjee, "A low-cost broadband millimeter-wave bias tee network using SICL technology," *Microwave and Optical Technology Letters*, vol. 65, no. 12, pp. 3171–3179, Aug. 2023, doi: <https://doi.org/10.1002/mop.33865>.
- [9] Y. Tu, *et al.*, "A Survey on Reconfigurable Microstrip Filter–Antenna Integration: Recent Developments and Challenges," *Electronics*, vol. 9, no. 8, pp. 1249–1249, Aug. 2020, doi: <https://doi.org/10.3390/electronics9081249>.
- [10] X. Liu, W. Zhang, D. Hao, and Y. Liu, "A Compact Broadband Folded Dipole Antenna Element with Ball Grid Array Packaging for New 5G Application," *Progress in Electromagnetics Research Letters*, 96, 113–119, Feb. 17, 202, <https://doi.org/10.2528/PIERL21010502>.
- [11] M. Velghe, *et al.*, "Protocol for Personal RF-EMF Exposure Measurement Studies in 5th Generation Telecommunication Networks," *Research Square (Research Square)*, Jun. 2020, doi: <https://doi.org/10.21203/rs.3.rs-34590/v1>.
- [12] A. A. Abdulbari, *et al.*, "New design of wideband microstrip branch line coupler using T-shape and open stub for 5G application," *International Journal of Power Electronics and Drive Systems/International Journal of Electrical and Computer Engineering*, vol. 11, no. 2, pp. 1346–1346, Feb. 2021, doi: <https://doi.org/10.11591/ijece.v11i2.pp1346-1355>.
- [13] S. I. Yahya *et al.*, "A new compact and low phase imbalance microstrip coupler for 5G wireless communication systems," *PLoS ONE*, vol. 18, no. 12, pp. e0296272–e0296272, Dec. 2023, doi: <https://doi.org/10.1371/journal.pone.0296272>.
- [14] N. A. M. Shukor and N. Seman, "5G planar branch line coupler design based on the analysis of dielectric constant, loss tangent and quality factor at high frequency," *Scientific Reports*, vol. 10, no. 1, Sep. 2020, doi: <https://doi.org/10.1038/s41598-020-72444-2>.
- [15] H. A. Abdulnabi, M. A. Shurij, and A. A. Sohrab, "A Modified Polygon Shaped Microstrip Patch Antenna Array for Ultra-Wideband Applications," *Control Systems and Optimization Letters*, vol. 1, no. 2, pp. 99–103, Jul. 2023, doi: <https://doi.org/10.59247/csol.v1i2.31>.
- [16] C. Yang, R. Wu, Z. Xiao, and W. Xu, "Design of Novel Ultra-wideband Slow-wave Microstrip Transmission Line," *Journal of Physics Conference Series*, vol. 2480, no. 1, pp. 012005–012005, Apr. 2023, doi: <https://doi.org/10.1088/1742-6596/2480/1/012005>.
- [17] M. Abide, *et al.*, "Simulation of an S-Band MILO with Adjustable Beam Dump," *Plasma*, vol. 2, no. 2, pp. 138–155, May 2019, doi: <https://doi.org/10.3390/plasma2020011>.
- [18] J.-M. Song, V.-S. Trinh, S. Kim, and J.-D. Park, "275 GHz Quadrature Receivers for THz-Band 6G Indoor Network in 130-nm SiGe Technology," *IEEE Access*, vol. 11, pp. 138540–138548, Jan. 2023, doi: <https://doi.org/10.1109/access.2023.3340023>.
- [19] Q.-Y. Wang, C. Xue, C. Dong, and Y.-H. Zhou, "Effects of defects and surface roughness on the vortex penetration and

vortex dynamics in superconductor–insulator–superconductor multilayer structures exposed to RF magnetic fields: numerical simulations within TDGL theory," *Superconductor Science and Technology*, vol. 35, no. 4, pp. 045004–045004, Jan. 2022, doi: <https://doi.org/10.1088/1361-6668/ac4ad1>.

- [20] K. Hossain *et al.*, "A Frequency-Reconfigurable Microstrip Antenna with Constant Dipole-Like Radiation Patterns Using Single Bias, Triple Varactor Tuning with Reduced Complexity," *Wireless Personal Communications*, vol. 123, no. 2, pp. 1003–1024, Sep. 2021, doi: <https://doi.org/10.1007/s11277-021-09167-8>.
- [21] Y. Rao, H. J. Qian, B. Yang, R. Gomez-Garcia, and X. Luo, "Dual-Band Bandpass Filter and Filtering Power Divider With Ultra-Wide Upper Stopband Using Hybrid Microstrip/DGS Dual-Resonance Cells," *IEEE Access*, vol. 8, pp. 23624–23637, Jan. 2020, doi: <https://doi.org/10.1109/access.2020.2970209>.
- [22] M. M. Fakharian, "A compact UWB antenna with dynamically switchable band-notched characteristic using broadband rectenna and DC-DC booster," *International Journal of Microwave and Wireless Technologies*, vol. 13, no. 10, pp. 1086–1095, Feb. 2021, doi: <https://doi.org/10.1017/s1759078721000027>.